Electronic Supplementary Material (ESI) for Nanoscale.


Supporting Information for

# Oxidized Co-Sn Nanoparticles as Long-Lasting Anode Materials for Lithium-Ion Batteries

Marc Walter,[a,b] Simon Doswald,[a,b] Frank Krumeich,[a] Meng He,[a,b] Roland Widmer,[c] Nicholas P. Stadie,[a,b, d] and Maksym V. Kovalenko*[a,b]

[a] Department of Chemistry and Applied Biosciences, ETH Zürich – Swiss Federal Institute of Technology Zürich, Vladimir Prelog Weg 1, 8093 Zürich (Switzerland)

[b] Empa-Swiss Federal Laboratories for Materials Science and Technology, Laboratory for thin films and photovoltaics, Überlandstrasse 129, 8600 Dübendorf (Switzerland)

[c] Empa-Swiss Federal Laboratories for Materials Science and Technology, Nanotech@surfaces Laboratory, Überlandstrasse 129, 8600 Dübendorf (Switzerland)

[d] Present address: Department of Chemistry and Biochemistry, Montana State University, 59717 Montana (United States)

[*] Prof. Dr. Maksym V. Kovalenko
E-mail: mvkovalenko@ethz.ch

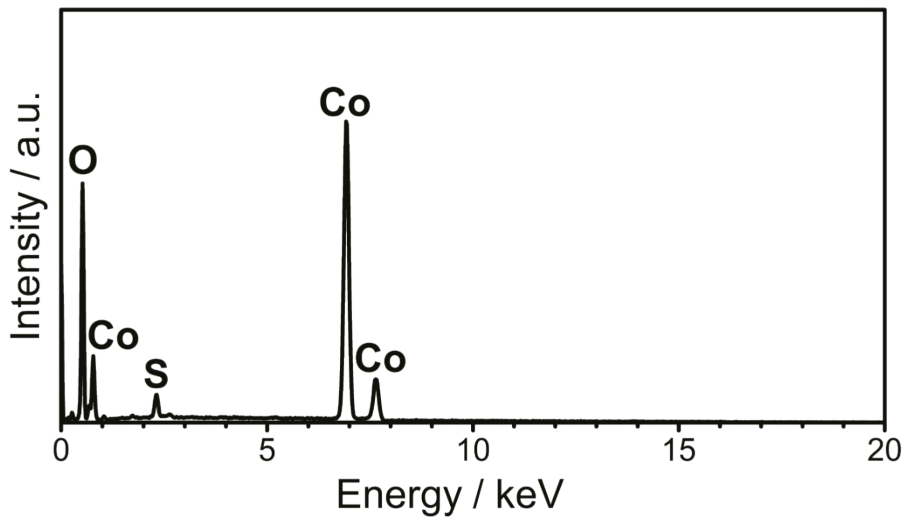


**Figure S1.** EDX spectrum of amorphous Co NPs. The peak denoted as S (corresponding to ~1 wt% of the sample) could be attributed to residual DMSO, left over after washing.

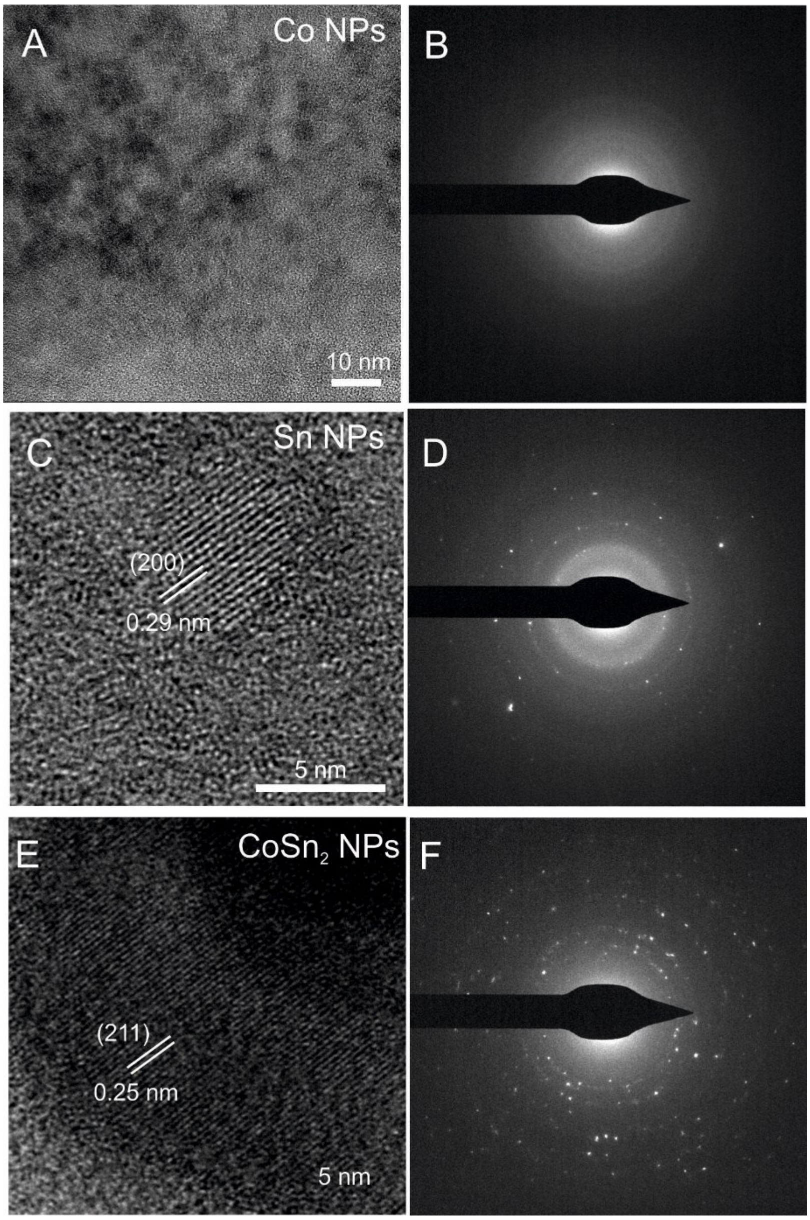


**Figure S2.** HR-TEM images along with selected area electron diffraction (SAED) and d-spacing of Co NPs (a, b), Sn NPs (c, d) and $CoSn_2$ NPs (e, f).

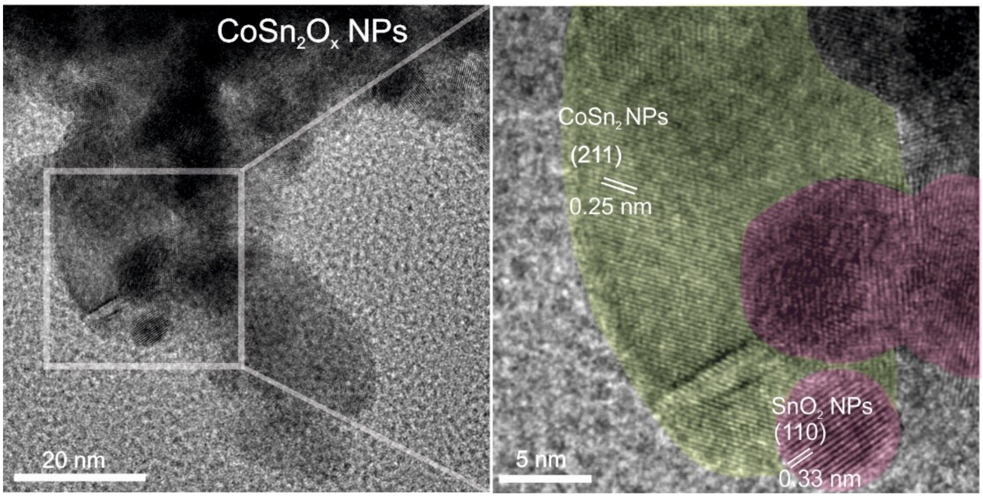


**Figure S3.** HR-TEM images of $CoSn_2O_x$ NPs with d-spacing.

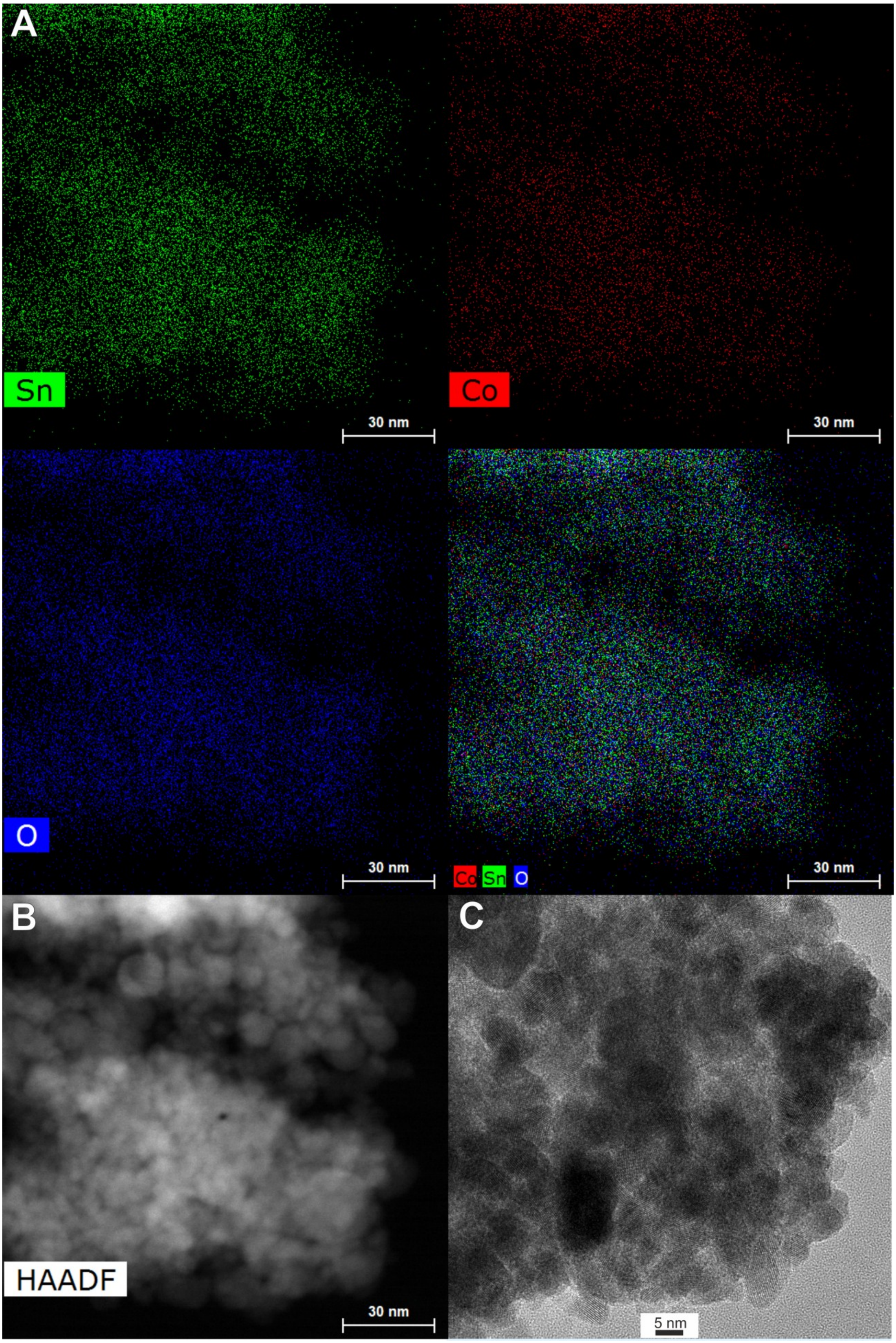


**Figure S4.** (A) Elemental EDX-STEM maps, (B) HAADF-STEM, and (C) HR-TEM images of $CoSn_2O_x$ NPs.

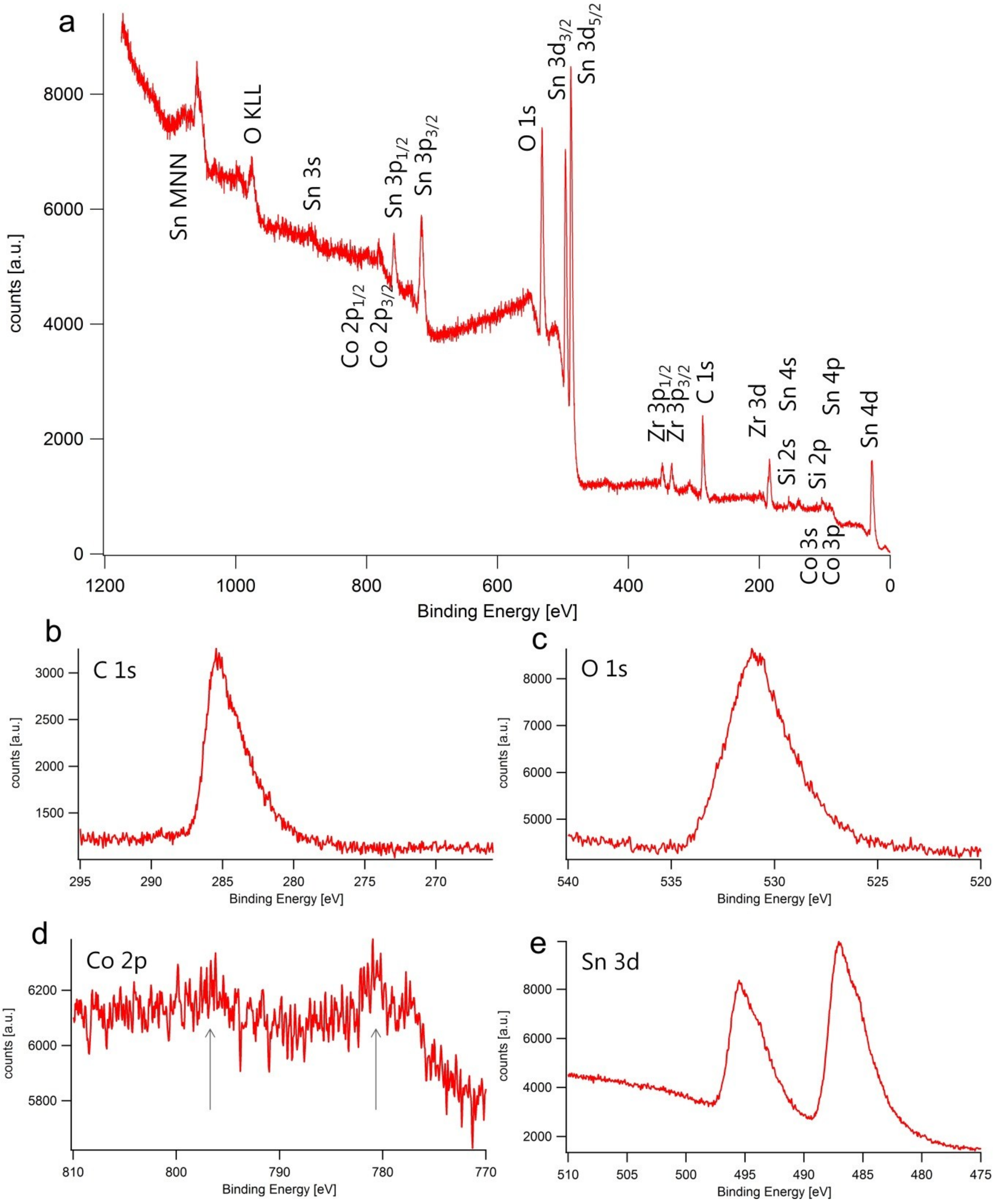


**Figure S5.** (a) XPS spectra of $CoSn_2O_x$ NPs. Survey spectrum assigning the peaks to the elements according to https://srdata.nist.gov/xps/EnergyTypeValSrch.aspx. Detail spectra of (b) C 1s, (c) O 1s, (d) Co 2p and (e) Sn 3d, where oxygen as well as carbon show two components, but more important, cobalt and tin are completely oxidized, most probably forming $Co(OH)_2$ and $SnO_2$ as follows form a ca. 3 eV and 1.7 eV shift of the individual peaks, respectively.

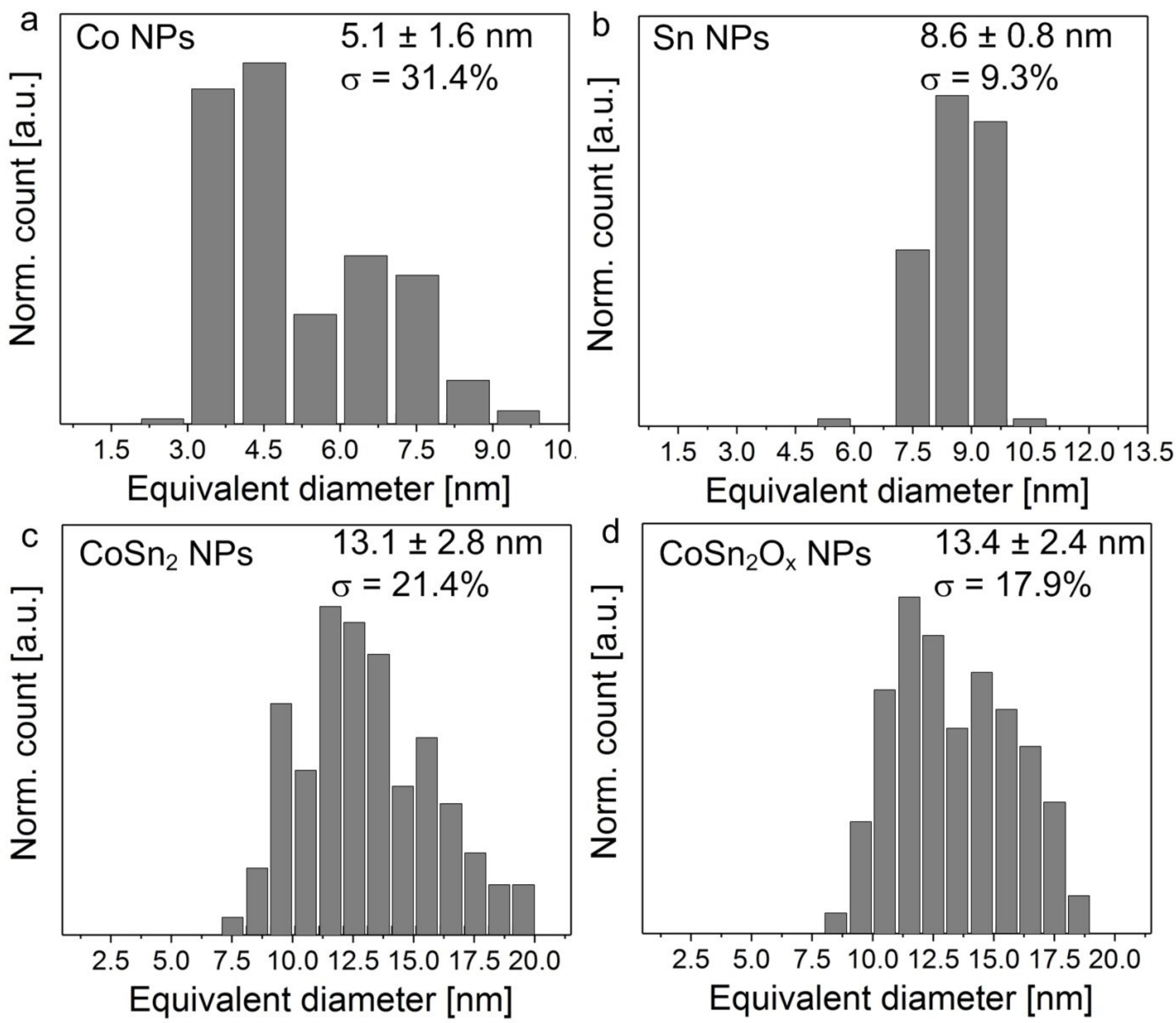


**Figure S6.** Size-distribution histograms of (a) Co NPs, (b) Sn NPs, (c) $CoSn_2$ NPs and (d) $CoSn_2O_x$ NPs. Mean sizes and standard deviations of nanoparticles were determined using PEBBLES (Mondini et al., *Nanoscale*, **2012**, *4*, 5356-5372).

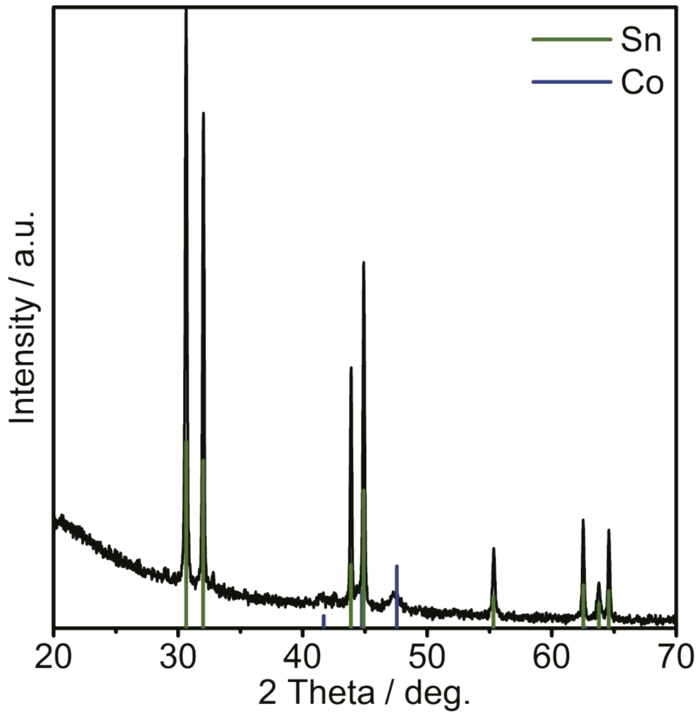


**Figure S7.** XRD pattern of a mixture of bulk Co and Sn powders (molar ratio 1:2) after ball-milling for 4 hours under nitrogen. All reflections can be indexed as belonging to Sn (ICDD PDF entry No.: 00-004-0673) or Co (ICDD PDF entry No.: 00-005-0727).

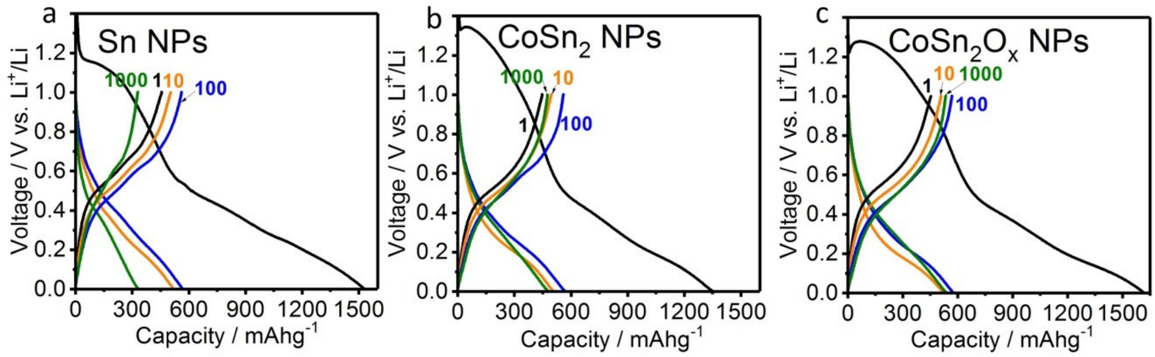


**Figure S8.** Galvanostatic charge/discharge curves with full capacity range for (a) Sn NPs, (b) $CoSn_2$ NPs, and (c) $CoSn_2O_x$ NPs measured during 1st, 10th, 100th and 1000th cycle at a current density of 1984 mA $g^{-1}$.

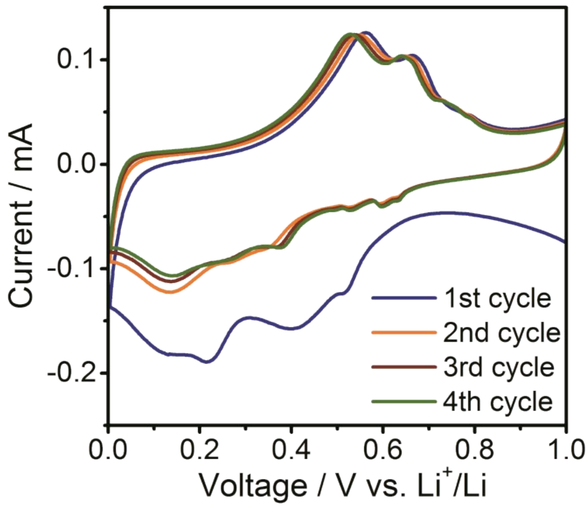


**Figure S9.** Cyclic voltammograms of crystalline Sn NPs in a lithium-ion half-cell using a scan rate of 0.1 mV $s^{-1}$ in the potential range of 0.005–1.0 V.

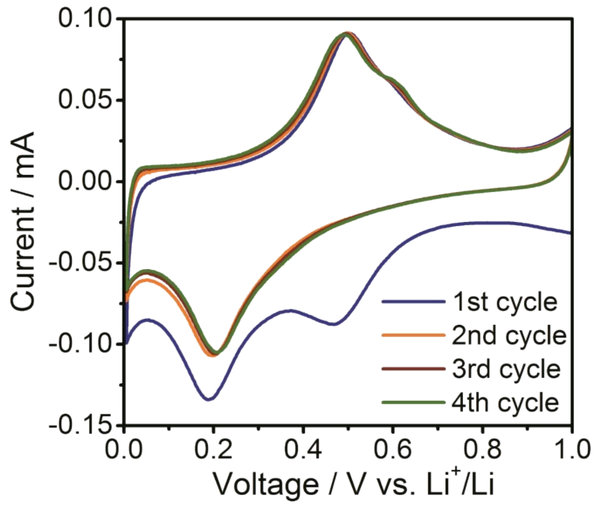


**Figure S10.** Cyclic voltammograms of $CoSn_2$ NPs in a lithium-ion half-cell using a scan rate of 0.1 mV $s^{-1}$ in the potential range of 0.005–1.0 V.

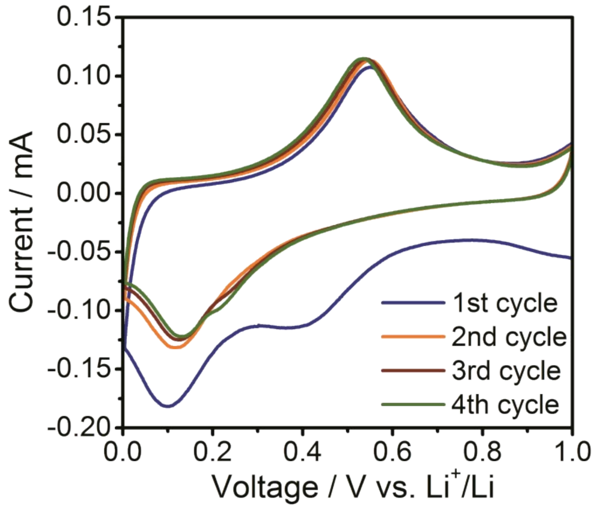


**Figure S11.** Cyclic voltammograms of $CoSn_2O_x$ NPs in a lithium-ion half-cell using a scan rate of 0.1 mV $s^{-1}$ in the potential range of 0.005–1.0 V.

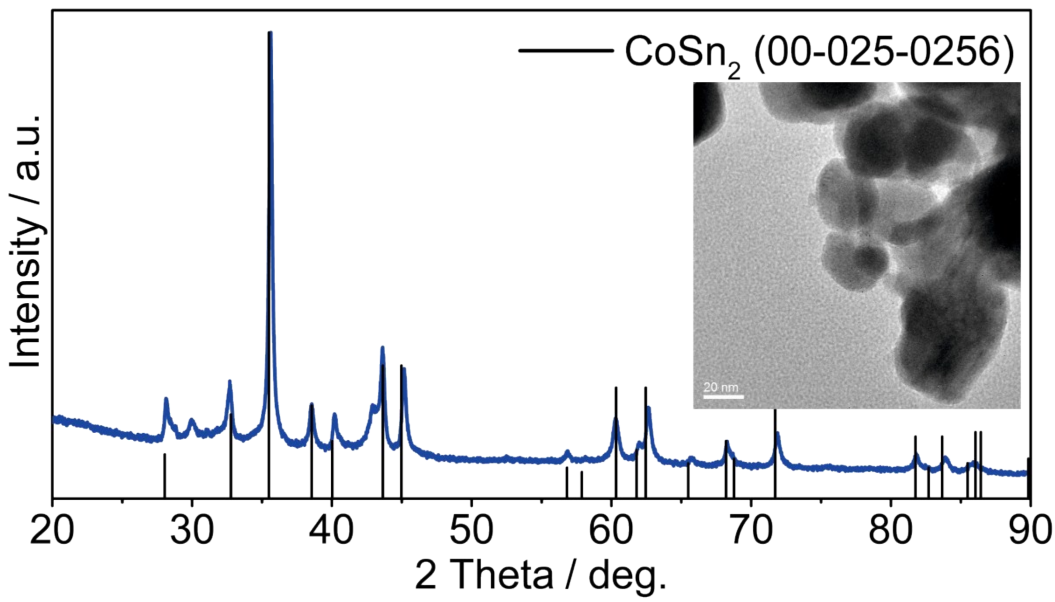


**Figure S12.** XRD pattern (with TEM image as inset) of $CoSn_2$ NPs prepared by wet-chemical synthesis. The two unindexed peaks at 30° and 43° might correspond to SnO and CoO. For synthesizing $CoSn_2$ NPs wet-chemically $SnCl_2$ (1.33 mmol) and $CoCl_2$ (0.67 mmol) dissolved in NMP (3 mL) were injected into a solution of $NaBH_4$ in NMP (16 mmol in 17 mL) at 150 °C and kept at this temperature for 1 hour.

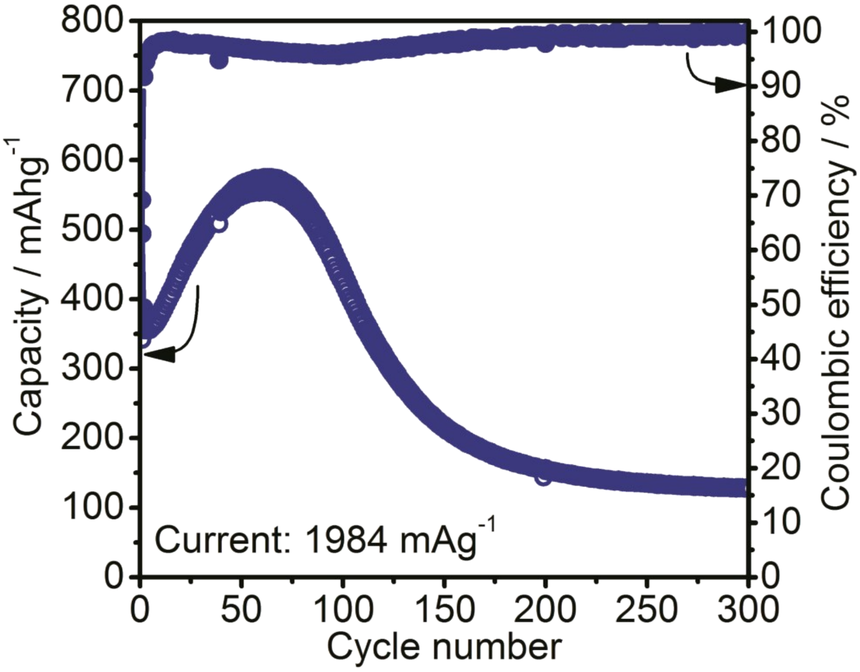


**Figure S13.** Cycling stability of $CoSn_2$ NPs prepared by wet-chemical synthesis in lithium-ion half-cells using a current of 1984 mA $g^{-1}$ in the potential range of 0.005–2.0 V.

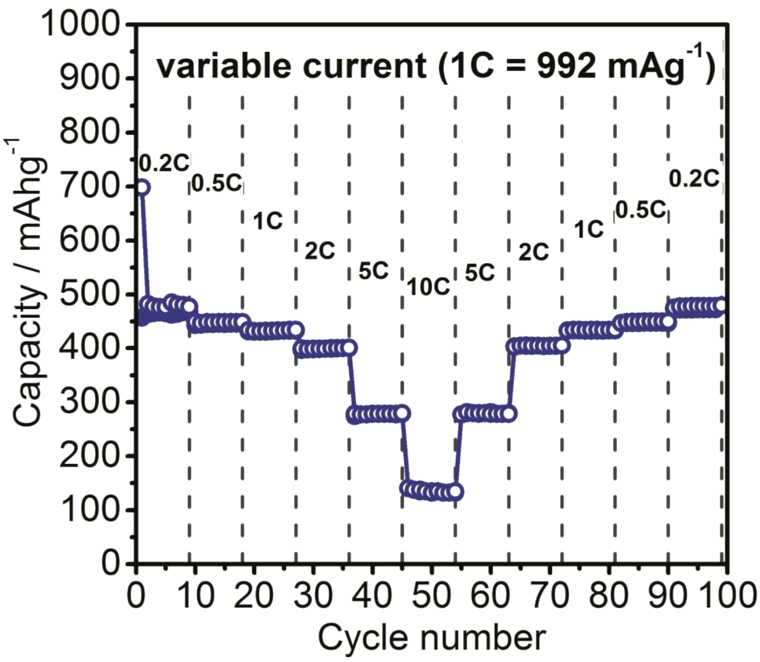


**Figure S14.** Rate capability tests for graphite in lithium-ion half-cells within the potential range of 0.005–1.0 V using the same conditions as for Co-Sn-based NPs in Figure 4.

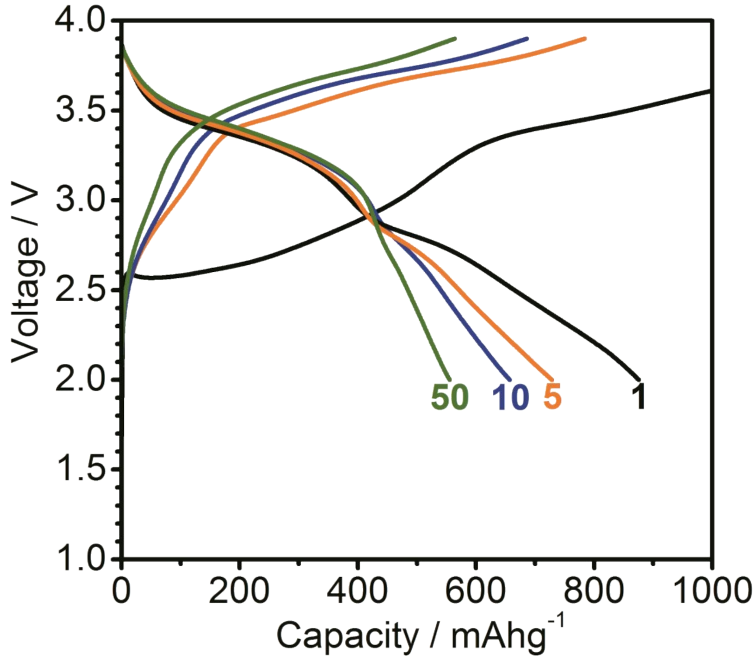


**Figure S15.** Galvanostatic charge/discharge curves for a $CoSn_2O_x/LiCoO_2$ full-cell. Cells were cycled with a current of 500 mA $g^{-1}$ in the potential range of 2.0–3.9 V. The specific capacities and currents correspond to the mass of the $CoSn_2O_x$ NPs.

**Table S1.** Comparison of the electrochemical performance of $CoSn_2O_x$ NPs (present work) with other reported systems as anode materials for LIBs.

| **Anode material** | **Current density ($mAg^{-1}$)** | **Initial capacity ($mAhg^{-1}$)** | **Retained capacity ($mAhg^{-1}$)** | **Cycle number** | **Potential range (V vs. $Li^+/Li$)** |
|---|---|---|---|---|---|
| $CoSn_2O_x$ NPs (present work) | 1984 | 450 (570 at cycle 100) | 525 | 1500 | 0.005–1.0 V |
| $CoSnO_3$@GN[1] | 2000 | ~708 | 566 | 1500 | 0.005–3.0 V |
| Co–Sn/carbon nanofibers composite[2] | 161 | 700 | 560 | 80 | 0.02–2.8 V |
| SnFeCo alloy composite[3] | 50 | 585 | 507 | 50 | 0.02–1.5 V |
| $Co_3Sn_2$@Co/nitrogen doped graphene[4] | 250 | 1600 | 1615 | 100 | 0.005–3 V |

| | | | | | |
|---|---|---|---|---|---|
| CoSn*x*@C–PAn[5] | 200 | 2038 | 2038 | 100 | 0.005–3 V |
| meso-Co0.3Sn0.7[6] | 50 | 663 | 530 | 50 | 0.001–2.0 V |
| Sn–Co nanoalloy embedded in porous N-doped carbon[7] | 2000 | 472 | 472 | 500 | 0.01–3V |
| Sn-Co-graphene composites[8] | 500 | 672 | 560 | 60 | 0.01–3 V |
| nano Sn-C[9] | 3000 | ~450 (at cycle 50) | 536.5 | 1000 | 0.01–2.5 V |
| nano Sn-C[10] | 4000 | ~390 | 410 | 1000 | 0.02–3.0 V |
| nano Sn-C[11] | 200 | 757 | 722 | 200 | 0.01–2.0 V |
| $Ni_3Sn_2$ microcages[12] | 570 | ~304 | ~304 | 1000 | 0.01–2.0 V |
| Sn NCs[13] | 1000 | ~800 | 550 | 100 | 0.005–2.0 V |
| nano Sn-C[14] | 200 | ~710 | ~710 | 130 | 0–3.0 V |
| Sn-carbon/silica[15] | 300 | ~440 | ~440 | 100 | 0–2.5 V |

**Table S2.** Comparison of the theoretical volumetric capacities for graphite or $CoSn_2O_x$-based anodes in full-cells with $LiCoO_2$ cathode.

| System | Capacity [mAh/g] | Density [g/cm$^3$] | Vol. capacity [mAh/cm$^3$] | Vol. cell capacity [mAh/cm$^3$] | Discharge voltage [V] | Vol. energy density [Wh/L] |
|---|---|---|---|---|---|---|
| **Graphite/$LiCoO_2$** | 372/140 | 2.2/5.1 | 818/714 | 381 | 3.55 | 1353 |
| **$CoSn_2O_x$/$LiCoO_2$** | 576/140 | 7.6*/5.1 | 4378/714 | 614 | 3.15 | 1934 |

*based on the bulk densities of Sn (7.3 g/cm$^3$) and Co (8.9 g/cm$^3$).

## References


1. C. Wu, J. Maier and Y. Yu, *Adv. Funct. Mater.*, 2015, **25**, 3488-3496.
2. B.-O. Jang, S.-H. Park and W.-J. Lee, *J. Alloys Compd.*, 2013, **574**, 325-330.
3. X. Li, X. He, Y. Xu, L. Huang, J. Li, S. Sun and J. Zhao, *J. Mater. Chem. A*, 2015, **3**, 3794-3800.
4. N. Mahmood, C. Zhang, F. Liu, J. Zhu and Y. Hou, *ACS Nano*, 2013, **7**, 10307-10318.
5. N. Mahmood, J. Zhu, S. Rehman, Q. Li and Y. Hou, *Nano Lett.*, 2015, **15**, 755-765.
6. G. O. Park, J. Yoon, J. K. Shon, Y. S. Choi, J. G. Won, S. B. Park, K. H. Kim, H. Kim, W.-S. Yoon and J. M. Kim, *Adv. Funct. Mater.*, 2016, **26**, 2800-2808.
7. X. Shi, H. Song, A. Li, X. Chen, J. Zhou and Z. Ma, *J. Mater. Chem. A*, 2017, **5**, 5873-5879.
8. J. Zhu, D. Wang, T. Liu and C. Guo, *Electrochim. Acta*, 2014, **125**, 347-353.
9. X. Huang, S. Cui, J. Chang, P. B. Hallac, C. R. Fell, Y. Luo, B. Metz, J. Jiang, P. T. Hurley and J. Chen, *Angew. Chem. Int. Ed.*, 2015, **54**, 1490-1493.
10. N. Zhang, Q. Zhao, X. Han, J. Yang and J. Chen, *Nanoscale*, 2014, **6**, 2827-2832.
11. Z. Zhu, S. Wang, J. Du, Q. Jin, T. Zhang, F. Cheng and J. Chen, *Nano Lett.*, 2014, **14**, 153-157.
12. J. Liu, Y. Wen, P. A. van Aken, J. Maier and Y. Yu, *Nano Lett.*, 2014, **14**, 6387-6392.
13. K. Kravchyk, L. Protesescu, M. I. Bodnarchuk, F. Krumeich, M. Yarema, M. Walter, C. Guntlin and M. V. Kovalenko, *J. Am. Chem. Soc.*, 2013, **135**, 4199-4202.
14. Y. Xu, Q. Liu, Y. Zhu, Y. Liu, A. Langrock, M. R. Zachariah and C. Wang, *Nano Lett.*, 2013, **13**, 470-474.
15. J. Hwang, S. H. Woo, J. Shim, C. Jo, K. T. Lee and J. Lee, *ACS Nano*, 2013, **7**, 1036-1044.